T Cells Play a Causal Role in Diastolic Dysfunction during Uremic Cardiomyopathy

Pamela D. Winterberg,[1,2] Jennifer M. Robertson,[3] Michael S. Kelleman,[4] Roshan P. George,[1,2] and Mandy L. Ford[3]

[1]Division of Pediatric Nephrology, Department of Pediatrics, [3]Emory Transplant Center, Department of Surgery, and [4]Biostatistics Core, Department of Pediatrics, Emory University School of Medicine, Atlanta, Georgia; and [2]Children's Healthcare of Atlanta, Atlanta, Georgia

ABSTRACT

Background Uremic cardiomyopathy, characterized by left ventricular hypertrophy, diastolic dysfunction, and impaired myocardial strain, contributes to increased cardiovascular mortality in patients with CKD. Emerging evidence suggests a pathogenic role for T cells during chronic heart failure.

Methods To determine whether T cells contribute to uremic cardiomyopathy pathogenesis, we modeled this condition by inducing CKD *via* 5/6th nephrectomy in mice. We used flow cytometry to assess expression of markers of T cell memory or activation by lymphocytes from CKD mice and controls, as well as lymphocyte capacity for cytokine production. Flow cytometry was also used to quantify immune cells isolated from heart tissue. To test effects of T cell depletion on cardiac function, we gave CKD mice anti-CD3 antibody injections to deplete T cells and compared heart function (assessed by echocardiography) with that of controls. Finally, we correlated T cell phenotypes with structural and functional measures on clinically acquired echocardiograms in children with CKD.

Results Mice with CKD accumulated T cells bearing markers of memory differentiation ($CD44^{hi}$) and activation (PD-1, KLRG1, OX40), as reported previously in human CKD. In addition, mice with CKD showed T cells infiltrating the heart. T cell depletion significantly improved both diastolic function and myocardial strain in CKD mice without altering hypertension or degree of renal dysfunction. In children with CKD, increasing frequency of T cells bearing activation markers PD-1 and/or CD57 was associated with worsening diastolic function on echocardiogram.

Conclusions CKD results in an accumulation of proinflammatory T cells that appears to contribute to myocardial dysfunction.

J Am Soc Nephrol 30: 407–420, 2019. doi: https://doi.org/10.1681/ASN.2017101138

Uremic cardiomyopathy, characterized by left ventricular hypertrophy (LVH), diastolic dysfunction, and impaired ventricular strain, is a common finding in children with CKD[1–4] and predicts mortality among adults with CKD.[5–7] However, the underlying mechanisms contributing to the development of uremic cardiomyopathy are complex and incompletely understood, limiting therapeutic approaches.

CKD represents a unique, nontraditional risk factor for cardiovascular disease. Biomarkers of inflammation, including circulating TNF, C-reactive protein, and IL-6, correlate with the structural and functional changes of uremic cardiomyopathy[8–11] and mortality[12–14] in the CKD population. In addition, loss of naïve T cells and accumulation of memory T cells[15,16] with proinflammatory cytokine secretion capacity[17–19] have been described in the peripheral blood of patients with CKD,

Received October 28, 2017. Accepted December 24, 2018.

Published online ahead of print. Publication date available at www.jasn.org.

Correspondence: Dr. Pamela D. Winterberg, Division of Pediatric Nephrology, Emory University School of Medicine, 2015 Uppergate Drive NE, Atlanta, GA 30345. Email: pdwinte@emory.edu

Copyright © 2019 by the American Society of Nephrology

and correlate with cardiovascular events[20,21] in this patient population. We have recently reported that children with CKD, despite their young age and limited antigen exposure, also accumulate memory T cells with similarly altered phenotypes.[22] Specifically, we found children have variably increased frequency of central and effector memory T cells bearing programmed cell death 1 (PD-1) or CD57, markers of sustained activation.

Emerging evidence now supports a pathogenic role for T cells during hypertension[23–25] and pressure overload–induced heart failure.[26–29] Here, we present several pieces of evidence supporting a causal role for T cells in the pathogenesis of uremic cardiomyopathy, potentially serving as a link between inflammation and cardiac remodeling during CKD.

Significance Statement

Uremic cardiomyopathy, which features left ventricular hypertrophy, diastolic dysfunction, and impaired myocardial strain, predicts mortality in patients with CKD. In this study, the authors present findings supporting emerging evidence that T cells play a causal role in diastolic dysfunction during CKD. In a mouse model of CKD, they demonstrate that T cells infiltrate the heart and lead to diastolic dysfunction and impaired ventricular strain, whereas depletion of T cells improves diastolic function and myocardial strain. They also show that in children with CKD, increasing frequency of T cells bearing markers of sustained activation (PD-1 and CD57) is associated with echocardiographic indications of worsening diastolic function. Future research may inform novel therapies that target T cell function to mitigate early subclinical myocardial dysfunction during CKD.

METHODS

Mouse CKD Model

CKD was induced in 5-week-old, male 129×1/SvJ mice (JAX) through 5/6th nephrectomy as previously described.[30] Age-matched mice undergoing bilateral sham surgeries served as controls. All animal experiments were conducted in accordance with the National Institutes of Health *Guide for the Care and Use of Laboratory Animals*, using protocols approved by Emory University Institutional Animal Care and Use Committee (protocol 2003480). T cell depletion experiments used 100 μg anti-CD3e antibody (InVivoPlus, clone 145–2C11; BioXcell, West Lebanon, NH) or isotype antibody (polyclonal Hamster IgG; BioXcell) administered *via* intraperitoneal injection every 3–4 days. Plasma urea (catalog no. K024-^{1}H; Arbor Assays, Ann Arbor, MI) and cystatin C (R&D Systems, Minneapolis, MN) concentrations were determined following manufacturer protocols.

Small-Animal Cardiovascular Evaluation

Transthoracic echocardiography (Vevo2100; VisualSonics, Toronto, Canada) was performed on mice under 1%–2% isoflurane anesthesia. Left ventricular diastolic function was assessed by measuring the wave ratio of the left ventricular transmitral early and late peak flow velocities (E/A ratio) of four or five averaged cardiac cycles from at least two scans per mouse. Ventricular strain analyses were conducted using speckle-tracking software (Vevostrain Analysis) as previously reported.[30] BP were measured using noninvasive tail-cuff measurements (BP-2000 BP Analysis System; Visitech Systems, Apex, NC) after a minimum of 5 days of behavioral acclimation.

RNA Sequencing

Mice (n=5 CKD, n=5 sham) were euthanized at 8 weeks after partial nephrectomy: hearts were flushed with PBS while still beating, and then removed. The left ventricle was isolated and preserved in RNA later overnight at 4°C, and stored at −80°C until processing for RNA. Total RNA isolation and complementary DNA libraries from murine hearts were constructed using standard methods on the basis of the Illumina TruSeq platform. Libraries were validated by microelectrophoresis, quantified, pooled and clustered on Illumina TruSeq v3 flowcells, and sequenced on an Illumina HiSeq 1000 in 100-base, single-read reactions. mRNA sequencing reads were aligned to the mm10 (University of California, Santa Cruz) mouse reference assembly and annotated using the STAR RNA-seq aligner (version 2.4.0f1).[31] Transcript assembly, abundance estimates, and differential expression analysis were performed using Cufflinks v2.1.1 and Cuffdiff.[32] Significant differential expression was determined using a Benjamini–Hochberg corrected false discovery rate of $<$0.05. Pathway analysis of differentially expressed genes was performed was performed in Ingenuity Pathway Analysis software (Qiagen) with platform-defined reference background. The significance of the pathways was determined on the basis of the ratio of differentially expressed genes within each pathway and the Fisher exact test ($P<0.05$). Heatmaps were created for data visualization (Partek Genomics Suite) for pathways of interest. Gene expression was log-transformed ($\log_2(x+0.001$ offset) to normalize to baseline. Unsupervised hierarchical clustering was performed using all differentially expressed genes in the pathways of interest to sort the samples. As a control, pathway and gene ontology analysis for differentially expressed genes was performed using open-source software (DAVID) and Ingenuity Pathway Analysis against the user dataset as reference (see Supplemental Appendices 1–7).

Isolation of Cardiac Immune Cells

Hearts were collected at 2 weeks after induction of CKD for flow cytometry analysis. Hearts were flushed *in situ* with PBS injected *via* the right ventricle. The left ventricle was then dissected, weighed, cut into pieces, and digested in RPMI containing 0.12 mg/dl of Liberase TM (Roche) for 10 minutes at 37°C with vigorous stirring (280 rpm). Supernatant was then added to 10 ml of ice-cold RPMI supplemented with 10% FBS. Two milliliters of fresh digestion buffer were then added to remaining tissue fragments and incubated for an additional 10 minutes. Cell suspensions were then pooled and washed in fresh RPMI plus 10% FBS, then passed through a 40-μm cell

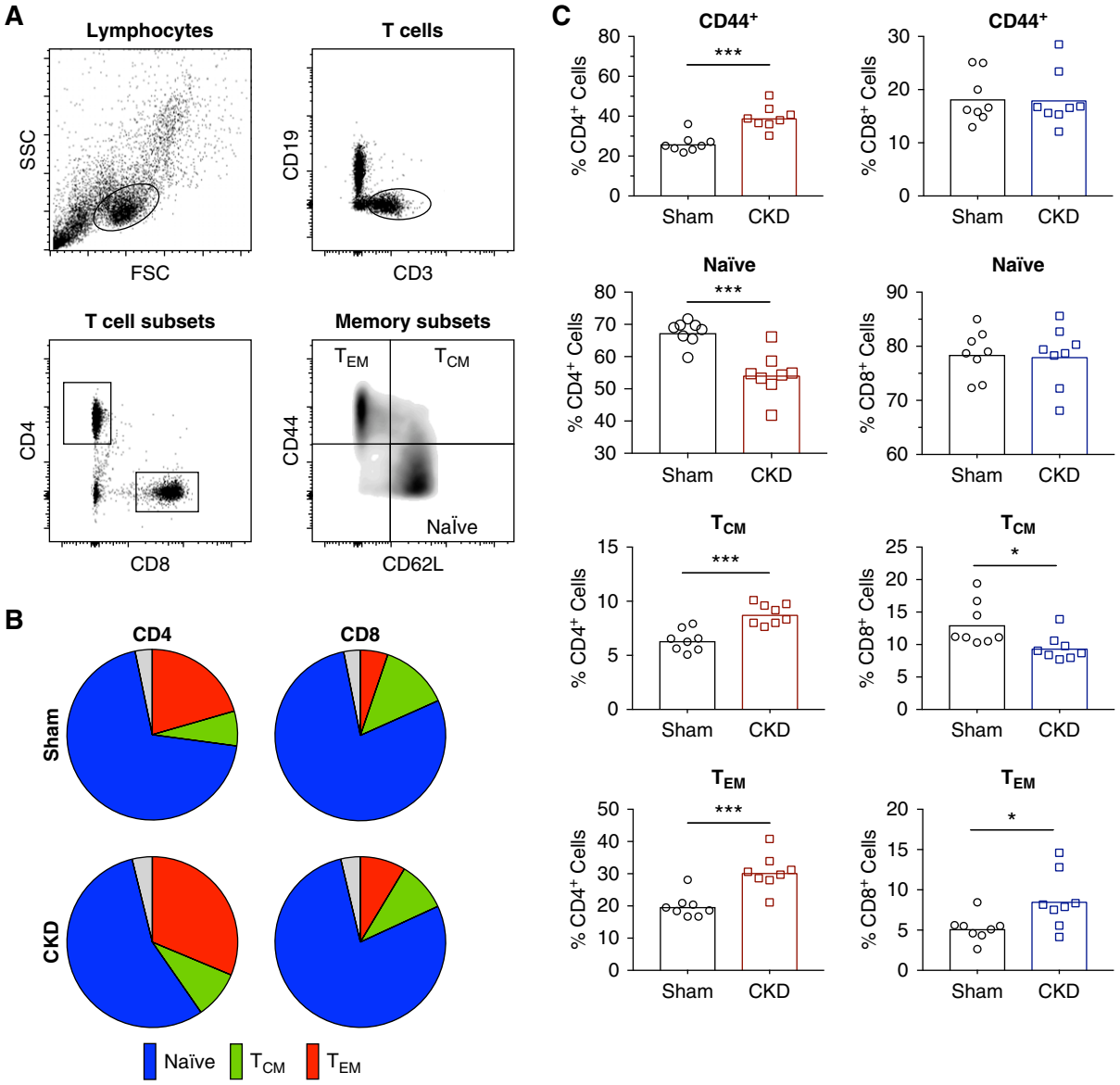

Figure 1. Mice with CKD accumulate memory T cells. (A) Gating strategy for T cell memory subsets. T_{EM} (effector memory cells) are $CD44^+CD62L^-$, T_{CM} (central memory cells) are $CD44^+CD62L^+$, and naïve cells are $CD44^-CD62L^-$. (B) Comparison of relative frequencies of memory subsets for CD4 and CD8 T cells between sham-operated and CKD mice. (C) Frequency of memory subsets for $CD4^+$ and $CD8^+$ T cells from spleen are compared between sham-operated and CKD mice. Data are representative of three independent experiments. *$P<0.05$; ***$P<0.001$.

strainer and stained for flow cytometry (see Table 1 in Supplemental Appendix 8).

Flow Cytometry and viSNE Analysis

Single-cell suspensions from peripheral blood or spleen of mice were stained with fluorophore-conjugated monoclonal antibodies (see Table 1 in Supplemental Appendix 8), interrogated using an LSRII flow cytometer (BD Biosciences) and analyzed using FlowJo software (Treestar). T cell memory subsets were defined by expression of CD44 and CD62L as described in Figure 1. Frequency of $PD1^{hi}$, $KLRG1^{hi}$, and $OX40^{hi}$ were determined for $CD4^+$ and $CD8^+$ populations using negative gates defined by "fluorescent minus one" stained samples. CountBright beads (Life Technologies) were used to quantify volume analyzed for blood, lymph node, and heart samples. Flow cytometry standard files generated from pregating on total T cells ($CD3^+CD19^-$) were imported into the Cytobank online platform (www.cytobank.org) for viSNE[33] analyses of high-dimensional flow cytometry data. The viSNE algorithm generates two additional variables for each cell, the tSNE components, after nonlinear dimensionality reduction of multicolor flow data using t-stochastic neighbor

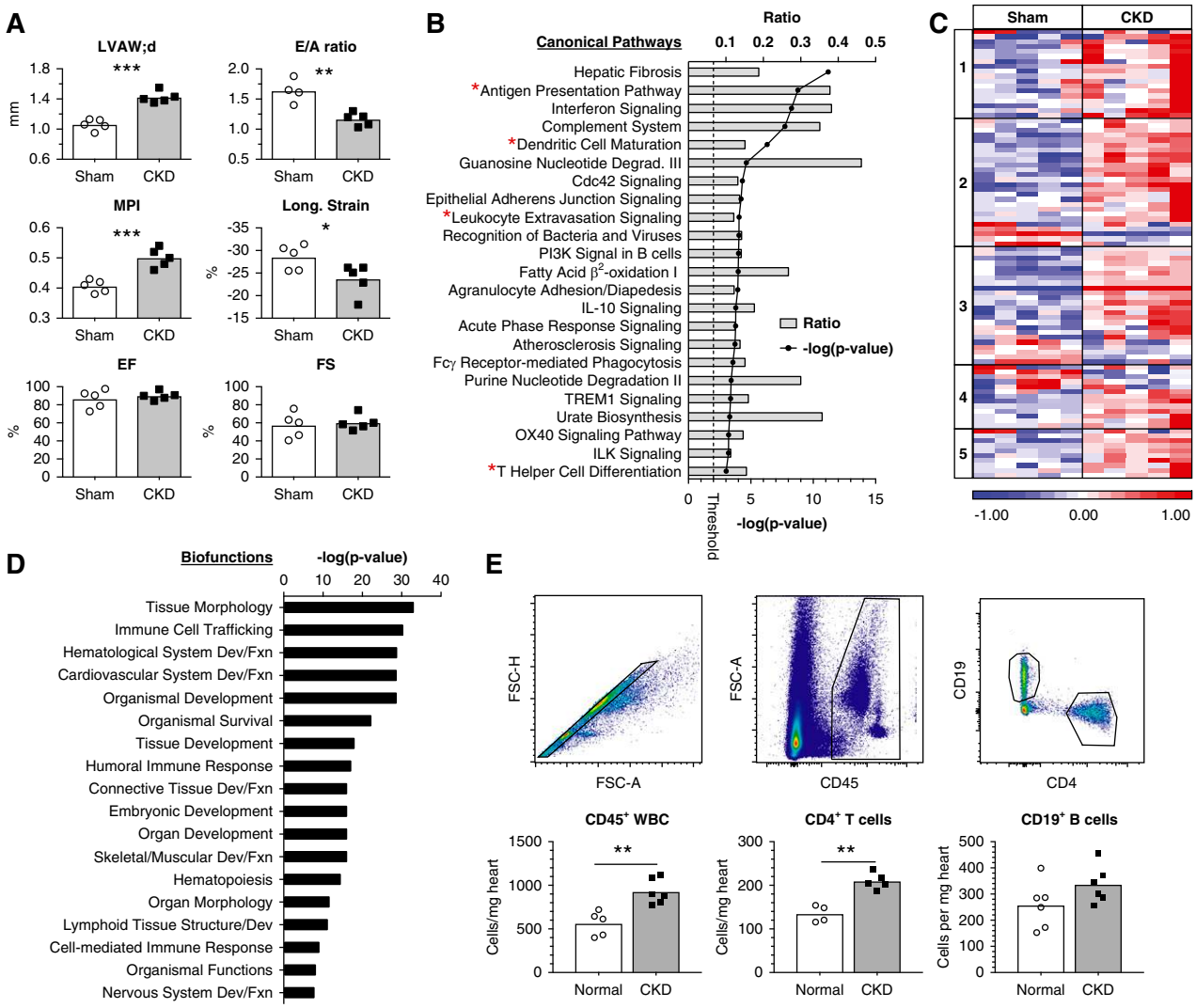

Figure 2. Hearts of mice with CKD have genetic signature of adaptive immune response and infiltration of T cells. Mice underwent cardiovascular phenotyping at 8 weeks after 5/6th nephrectomy (CKD, *n*=5) or sham surgery (*n*=5), followed by heart isolation for gene expression. (A) Echocardiography demonstrates LVH (increased LVAW;d), diastolic dysfunction (decreased E/A ratio and increased MPI), and impaired myocardial deformation (longitudinal strain), but normal systolic function (EF and FS). Heart tissue from mice in (A) were processed for RNA isolation and sequenced and subsequently analyzed for changes differential expression on the basis of (D) biofunction group and (B) canonical pathways using the Ingenuity analysis platform. (C) Heatmap shows relative expression of individual within pathways of the adaptive immune response between hearts from sham-operated and CKD mice: (*1*) antigen presentation, (*2*) dendritic cell maturation, (*3*) leukocyte extravasation, (*4*) T cell costimulatory signaling, and (*5*) helper T cell differentiation. (E) Flow cytometry analysis of hearts from mice demonstrate increased leukocytes, including $CD4^+$ T cells in the hearts of mice with CKD. **P*<0.05; ***P*<0.01; ****P*<0.001. Dev/Fxn, development and function; EF, ejection fraction; FS, fractional shortening; LV, left ventricle; LVAW;d, diastolic left ventricle anterior wall thickness; MPI, myocardial performance index; WBC, white blood cells.

embedding (t-SNE). The t-SNE components are then visualized on a two-dimensional dot plot (t-SNE map) to enable pattern recognition of the unsupervised clustering of cells.

Ex Vivo Stimulation and Intracellular Cytokine Staining

Isolated splenocytes were plated at 1×10^6 cells per well in RPMI 1640 media supplemented with 10% heat-inactivated FBS, 1% L-glutamine, 1% penicillin/streptomycin, 1% 2-mercaptoethanol, and 1 μg/ml of Brefeldin A, and then incubated at 37°C for 4 hours in the presence or absence of PMA (Sigma, St. Louis, MO) and ionomycin (Sigma) at a concentration of 1 μg/ml each. Intracellular cytokine staining was performed after fixation and permeabilization (BioLegend, San Diego, CA) using fluorescence-labeled antibodies against IFNγ, TNF, and IL-2 (see Table 1 in Supplemental Appendix 8).

Pediatric CKD T Cell Phenotype and Echo Correlation

T cell memory phenotypes and expression of CD57 and PD-1 were previously reported in a cross-sectional observational study of children with CKD (ClinicalTrials.gov identifier: NCT01283295).[22] Memory cell subsets were defined by expression of CCR7 and CD45RA (naïve $CD45RA^{+}CCR7^{+}$, central memory $CD45RA^{-}CCR7^{+}$, effector memory $CD45RA^{-}CCR7^{-}$, and effector memory RA $CD45RA^{+}CCR7^{-}$) as previously described.[34] Charts were reviewed and participants with clinically acquired echocardiograms during the study period identified. Echocardiographic reports and images were reviewed for completeness. Echocardiogram studies with complete assessment of diastolic function (*e.g.*, Doppler images) were included for further analysis (see Figure 3 in Supplemental Appendix 8). Spearman correlation analyses were performed using SAS Version 9.4 for Windows (SAS Institute Inc., Cary, NC) to assess for associations between flow cytometry phenotypes (frequencies of T cell memory subsets, CD57 expression, and/or PD-1 expression) and continuous variables for cardiac structure or function. Diastolic function was assessed by the ratio of early diastolic transmitral flow (E) to early diastolic mitral annular tissue (e') velocities on Doppler (E/e' ratio).[35] For cardiac structure, we used the SD score (*z* score) for sex and age of the height-indexed left ventricular mass (measured as grams per meter$^{2.7}$).[36] The limited sample size precluded multivariable correlations and assessment of confounding variables.

RESULTS

T Cells Infiltrate the Hearts of CKD Mice

We first set out to characterize transcriptional changes in the left ventricles of mice with CKD to identify differentially regulated inflammatory pathways. As we have previously reported,[30] mice with CKD display LVH and diastolic dysfunction with preserved systolic function (see Figure 2A). RNA sequencing of hearts from mice with uremic cardiomyopathy yielded over 1000 differentially expressed mRNA transcripts compared with hearts from age-matched, sham-operated mice (see Supplemental Appendices 1–7). Interestingly, Ingenuity biofunctions analysis identified significant enrichment for genes involved in immune processes (Figure 2D), including immune cell trafficking, humoral immune response, and cell-mediated immune response. Furthermore, ten of the top 20 differentially expressed Ingenuity canonical pathways involved inflammation and immune system function (Figure 2B), including pathways needed for a T cell–mediated response: leukocyte extravasation, antigen presentation, dendritic cell maturation, T cell costimulatory signaling, and helper T cell differentiation (Figure 2, C and D). Finally, flow cytometry analysis of hearts from normal versus CKD mice showed increased numbers of leukocytes ($CD45^{+}$) per left ventricular mass, which were predominated by $CD4^{+}$ T cells (Figure 2E). In summary, T cells infiltrate the hearts of mice with CKD and heart transcripts from mice with CKD show differential expression of pathways needed for a T cell response, namely access to tissue, antigen presentation, and T cell costimulation.

Mice with CKD Accumulate T Cells with Memory Phenotype

We have previously reported that children with CKD have increased frequency of memory T cells expected for their age.[22] We next determined whether the CKD mouse model recapitulates the T cell alterations seen in patients with CKD. Flow cytometry analysis of spleen and peripheral blood lymphocytes revealed accumulation of $CD4^{+}$ memory T cells ($CD44^{hi}$) with concomitant decrease in naïve $CD4^{+}$ T cells (Figure 1, B and C). CKD mice also displayed increased frequency and absolute counts of both central memory ($CD44^{hi}CD62L^{+}$) and effector memory ($CD44^{hi}CD62L^{-}$) $CD4^{+}$ T cells. In contrast, the frequency and absolute counts (data not shown) of naïve versus memory $CD8^{+}$ T cells remained similar between CKD and sham-operated mice (Figure 1). However, CKD mice displayed a shift within the $CD8^{+}$ memory cell population toward the effector memory phenotype with fewer central memory cells than sham controls (Figure 1, B and C).

T Cells from Mice with CKD Display Markers of Sustained Activation and Increased Cytokine Secretion Potential

We next performed exploratory analysis of flow cytometry data using the viSNE computational program[33] to identify high-dimensional relationships of T cell phenotypic and activation markers between mice with and without CKD. The viSNE program allows visualization of high-dimensional flow cytometry data while maintaining cell-level statistics. Multiparameter flow cytometry data undergoes nonlinear dimensionality reduction *via* t-SNE to generate two additional variables for each cell, the tSNE components, which are then visualized on a two-dimensional dot plot (t-SNE map). The proximity of cells in the t-SNE map reflects their distance in high-dimensional space, thus cells with similar protein expression are clustered together, allowing identification of high-dimensional associations of markers that may be missed by conventional flow cytometry gating.[37] Individual protein markers detected by fluorescence-tagged antibodies are visualized *via* color scale in the t-SNE maps (see Figure 3A).

The viSNE analysis confirmed the redistribution of memory cell phenotypes between CKD and sham controls. Mice with CKD also displayed increased frequency of effector memory $CD4^{+}$ T cells ($CD44^{hi}CD62L^{lo}$) bearing killer cell lectin-like receptor subfamily G, member 1 (KLRG1), PD-1, and/or OX-40, suggestive of sustained antigen stimulation. The t-SNE maps also demonstrate that the expression of these three activation markers are not mutually exclusive nor completely overlapping and are mostly contained within the $CD4^{+}$ T cell effector and central memory populations. Using conventional flow cytometry gating, we confirmed a statistically significant

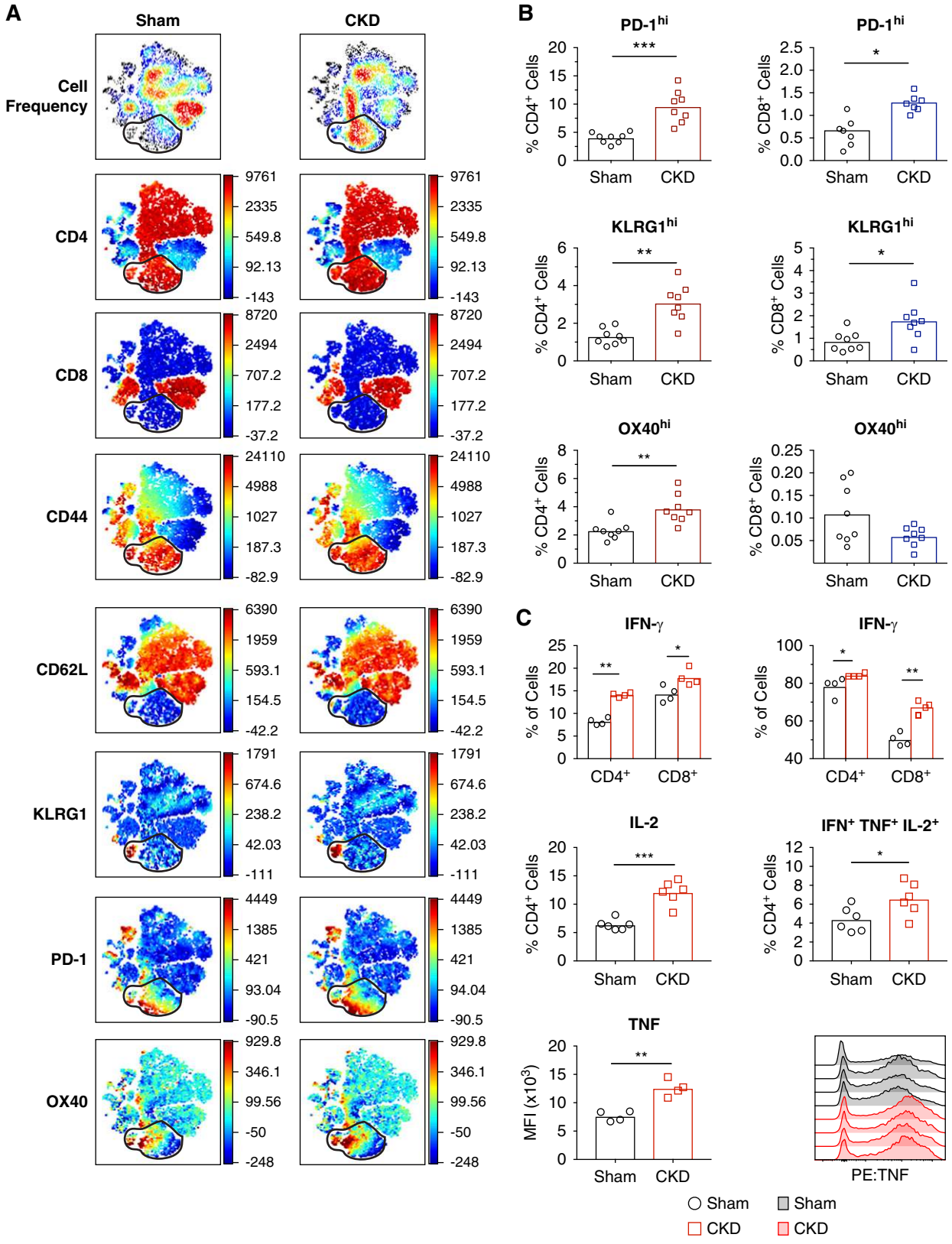

Figure 3. T cells from mice with CKD bear markers of activation and produce more cytokine in vitro after stimulation. (A) Representative t-SNE maps of flow cytometry data from T cells isolated from sham-operated versus CKD mice. The proximity of cells in the t-SNE map reflects their distance in high-dimensional space, thus cells with similar protein expression are clustered together. The color scale

increase in frequency of total $CD4^+$ T cells expressing KLRG, PD-1, or OX-40 (Figure 3B) in mice with CKD.

To explore the effect of CKD on T cell functionality, we assessed the capability of splenic T cells from mice with and without CKD to express cytokines after brief *ex vivo* stimulation. Stimulation resulted in increased frequency of both $CD4^+$ and $CD8^+$ T cells expressing TNF or IFNγ (Figure 3C) in mice with CKD compared with sham controls. There was also an increased frequency of $CD4^+$ T cells expressing IL-2. Furthermore, we found increased frequency of $CD4^+$ T cells with the capacity to simultaneously produce IL-2, TNF, and IFNγ in mice with CKD. Finally, the expression of TNF was higher in $CD4^+$ T cells from CKD mice as determined by increased median fluorescence intensity. Taken together, mice with CKD have profound systemic alterations in T cell memory and activation status with increased proinflammatory cytokine secretion capacity, similar to that previously reported in patients with CKD.

T Cell Depletion Ameliorates Diastolic Dysfunction in Mice with CKD

We next determined if T cells are mechanistically involved in the pathogenesis of uremic cardiomyopathy by testing the effect of T cell depletion on cardiac function in mice with CKD. Mice with CKD received injections of mAb directed against the pan-T cell marker CD3 (Figure 4A), and were compared with CKD and sham operated mice receiving injections of isotype-identical antibody to third-party antigens (isotype control). Anti-CD3 antibody treatment was successful in reducing the absolute number of $CD4^+$ and $CD8^+$ T cells in thoracic lymph nodes (Figure 4, C and E) by 4000- to 8000-fold, and in the spleen (Figure 4, D and F) by approximately 500-fold. In addition, thoracic lymph nodes, which are enlarged in CKD mice, were significantly reduced in mice receiving anti-CD3 antibody treatment (Figure 4B).

After 6 weeks of treatment, mice receiving anti-CD3 antibody showed improved diastolic function on echocardiography (Figure 4G), as indicated by increased E/A ratio, decreased myocardial performance index, and normalization of longitudinal strain, compared with CKD mice receiving isotype antibody injections. Measures of LVH including increased anterior wall thickness (1.392 ± 0.014 versus 1.452 ± 0.1366 mm; $P=0.30$) and increased left ventricular mass (117.2 ± 16.7 versus 113.8 ± 16.7 mg; $P=0.61$) were not improved in mice after T cell depletion, compared with CKD mice treated with isotype control. Furthermore, systolic BP, plasma urea concentration, and plasma cystatin C concentration were unaltered by T cell depletion (Figure 4H). We were unable to detect circulating TNF in the plasma of CKD mice treated with this antibody (see Figure 1 in Supplemental Appendix 8). Expression of type 1 collagen transcripts were not significantly different between sham and CKD mice (see Figure 2 in Supplemental Appendix 8). Expression of atrial natriuretic peptide and brain natriuretic peptide were not significantly different in CKD mice depleted of T cells (see Figure 2 in Supplemental Appendix 8). In summary, depletion of T cells in mice with CKD resulted in improved cardiac diastolic function independent of changes in LVH, BP, or renal function.

T Cell Subsets Correlate with Ventricular Function in Children with CKD

We next determined whether T cell activation and memory phenotypes are associated with cardiac function in patients with CKD by utilizing existing data from our previous observational study of T cell phenotypes in children with CKD.[22] Out of the 80 children for which we had T cell phenotyping, 51 had clinically acquired echocardiograms within 2 years of the study blood draw (see Figure 3 in Supplemental Appendix 8). Of these, 13 had echo studies with diastolic function assessment using the E/e' ratio. Demographic information of this subcohort can be found in Table 3 in Supplemental Appendix 8. Although limited in sample size, we found moderate-to-strong associations (Figure 5) between the accumulation of T cells bearing PD-1 and/or CD57 with worsening diastolic function (increasing E/e' ratio). Conversely, the accumulation of terminally differentiated effector memory $CD4^+$ T cells ($CCR7^-CD45RA^+$) showed a moderate association with improving diastolic function. In addition, we found moderate-to-strong associations between the loss of naïve $CD4^+$ or $CD8^+$ T cells or the accumulation of $CD4^+$ effector memory T cells with LVH. Finally, decreasing CD4:CD8 ratio, which is seen with continuous antigen stimulation or advanced aging, showed a moderate-to-strong association with worsening diastolic function and a modest association with increased left ventricular mass.

DISCUSSION

Cardiovascular disease remains a major cause of morbidity and mortality among children[38,39] and adults[40] with CKD, but the underlying mechanisms are incompletely understood and we remain without effective treatment[41–46] to improve outcomes.

in each map row represents the fluorescence intensity from high (red) to low (blue) for each antibody marker listed, except for the first row, which represents event (or cell) density within the sample. The area of the map representing the $CD4^+$ effector memory T cell population ($CD44^+CD62L^-$) is outlined for reference. (B) Quantitative representation of activation marker expression frequency within total CD4+ or CD8+ cell populations. (C) Cytokine expression as determined by intracellular staining and flow cytometry after *in vitro* stimulation. Data are representative of three independent experiments. *$P<0.05$; **$P<0.01$; ***$P<0.001$. MFI, median fluorescence intensity; OX40 (also known as CD134); PE, phycoerythrin.

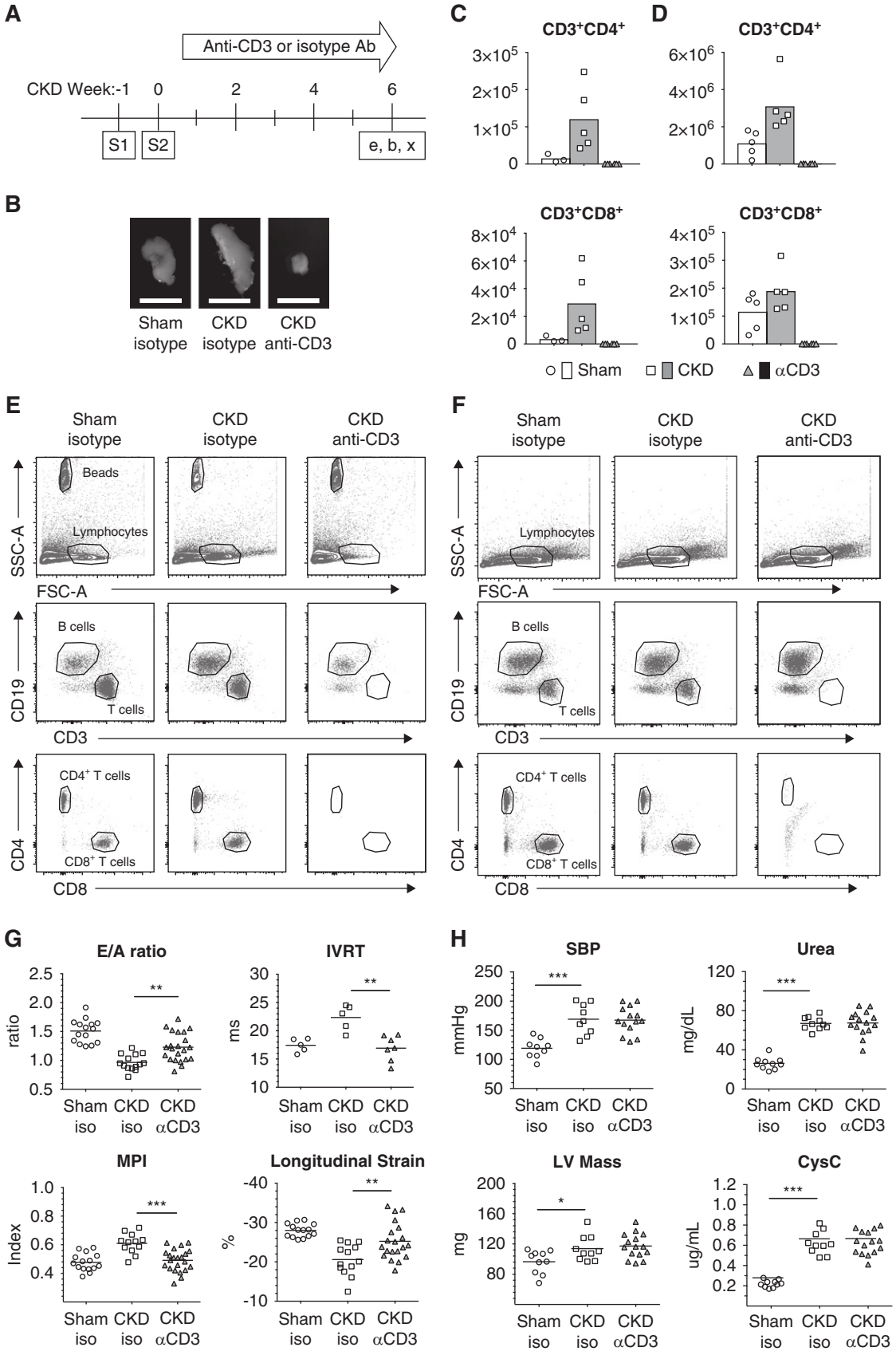
A
Anti-CD3 or isotype Ab
CKD Week:-1
0
2
4
6
S1
S2
e, b, x
B
Sham isotype
CKD isotype
CKD anti-CD3
C
CD3+CD4+
3×10^5
2×10^5
1×10^5
0
CD3+CD8+
8×10^4
6×10^4
4×10^4
2×10^4
0
D
CD3+CD4+
6×10^6
4×10^6
2×10^6
0
CD3+CD8+
4×10^5
3×10^5
2×10^5
1×10^5
0
Sham
CKD
αCD3
E
Sham isotype
CKD isotype
CKD anti-CD3
Beads
Lymphocytes
SSC-A
FSC-A
B cells
T cells
CD19
CD3
CD4+ T cells
CD8+ T cells
CD4
CD8
F
Sham isotype
CKD isotype
CKD anti-CD3
Lymphocytes
SSC-A
FSC-A
B cells
T cells
CD19
CD3
CD4+ T cells
CD8+ T cells
CD4
CD8
G
E/A ratio
ratio
2.5
2.0
1.5
1.0
0.5
**
Sham iso
CKD iso
CKD αCD3
IVRT
ms
30
25
20
15
10
**
Sham iso
CKD iso
CKD αCD3
MPI
Index
1.0
0.8
0.6
0.4
***
Sham iso
CKD iso
CKD αCD3
Longitudinal Strain
%
-40
-30
-20
-10
**
Sham iso
CKD iso
CKD αCD3
H
SBP
mmHg
250
200
150
100
50
***
Sham iso
CKD iso
CKD αCD3
Urea
mg/dL
120
80
40
0
***
Sham iso
CKD iso
CKD αCD3
LV Mass
mg
200
160
120
80
*
Sham iso
CKD iso
CKD αCD3
CysC
ug/mL
1.2
1.0
0.8
0.6
0.4
0.2
***
Sham iso
CKD iso
CKD αCD3

Uremic cardiomyopathy is a progressive cardiovascular complication in children[2,47] and adults with CKD[48–51] and is characterized by LVH and diastolic dysfunction. More recently, myocardial strain, which may signify subclinical cardiac dysfunction, has been shown to be impaired during early stages of CKD[4,52] and predicts risk for cardiovascular events[52] and mortality.[6,7,53]

In this report, we found several lines of evidence to support a role for T cells in the pathogenesis of diastolic dysfunction and impaired myocardial strain during uremic cardiomyopathy. First, T cells infiltrate uremic hearts early (2 weeks) in the uremic cardiomyopathy mouse model. In addition, next-generation RNA sequencing of uremic hearts identified enrichment for genes in pathways required for T cells to affect pathology, namely the recruitment, priming, and maturation of T cells. Furthermore, mice with CKD accumulate circulating memory T cell populations bearing costimulatory and coinhibitory receptors suggestive of repeated activation and displayed enhanced cytokine secretion capacity *in vitro*, similar to that described in patients with CKD.[15,16,22] Additionally, the frequency of T cells bearing markers of sustained activation (PD-1, CD57) correlated with diastolic function in children with CKD. Finally, we established a mechanistic role of T cells in uremic cardiomyopathy as diastolic function and myocardial strain improved when T cells were depleted in mice with CKD independent of any secondary effect of hypertension or degree of renal dysfunction. Taken together, CKD results in systemic accumulation of proinflammatory T cells that play a causal role in myocardial pathology.

Both diastolic dysfunction[54] and myocardial strain[7] predict mortality in adults and should therefore be considered clinically relevant outcomes in preclinical and translational studies of uremic cardiomyopathy. In clinical studies, diastolic dysfunction is often associated with LVH, resulting in a presumption that ventricular stiffness is secondary to thickening and/or fibrosis of the myocardium.[2,49] In our previous work,[30] we found that diastolic dysfunction and impaired myocardial strain in mice with CKD were actually detectable before the development of LVH on echocardiogram. Similarly, diastolic dysfunction has been shown to precede the development of both elevated BP and LVH during essential hypertension.[55–57]

T cell depletion in the mouse CKD model decoupled LVH from diastolic dysfunction as we observed improved diastolic indices (E/A ratio, isovolumic relaxation time, and myocardial performance index) and myocardial strain without changes in LVH. These data suggest that the diastolic dysfunction occurring in the mouse uremic cardiomyopathy model is independent of LVH. Furthermore, the observed effects of T cell depletion on myocardial performance in this model do not appear to be due to improvements in hypertension nor renal dysfunction.

Emerging evidence supports a pathogenic role for T cells in cardiac remodeling during pressure overload heart failure.[26–29] Two independent groups have reported improved myocardial structure and/or function after transaortic constriction (TAC) in mice strains lacking T cells. Laroumanie *et al.*[26] reported improved systolic function (measured by fractional shortening) and myocardial fibrosis after TAC in RAG2 knockout mice lacking both T cells and B cells, which were abrogated with reconstitution of $CD3^+$ T cells. Similarly, Nevers *et al.*[29] found reduced LVH, decreased myocardial fibrosis, and improved diastolic function after TAC in T cell α-receptor knockout mice compared with wild-type controls. We have not replicated the uremic cardiomyopathy model in mice with genetic T cell deficiency because of a lack of readily available knockouts on the S129 background. C57BL/6 mice are notoriously resistant to the development of hypertension, proteinuria, and glomerulosclerosis in the partial nephrectomy CKD model.[58,59] We have also observed that C57BL/6 mice not develop LVH, diastolic dysfunction, or impaired ventricular strain in the CKD model, and therefore did not pursue experiments evaluating uremic cardiomyopathy in the T cell–deficient strains reported by Laroumanie *et al.* and Nevers *et al.* Rather, we chose pharmacologic depletion in the S129×1/SvJ strain, which reliably reproduces the clinical features of uremic cardiomyopathy.[30,60] Interestingly, Nevers *et al.* reported that T cell depletion using anti-CD3 antibody treatment after TAC in wild-type C57BL/6 mice resulted in improved fractional shortening and reduced fibrosis, but no difference in LVH.

We have previously demonstrated that cardiac fibrosis is a late finding in the mouse CKD model (12–16 weeks of CKD).[31] In line with these previous observations, at 6 weeks, we found no difference in myocardial expression of natriuretic peptide or type 1 collagen genes (see Figure 2 in Supplemental

Figure 4. T cell depletion improves cardiac function in mice with CKD. (A) Experimental design. Mice with CKD were intraperitoneally injected (n=15) with depleting antibody against the pan-T cell marker, CD3, (anti-CD3) or isotype control (n=10) antibody every 3–4 days after 5/6th nephrectomy. Sham-operated mice received isotype control antibody (n=10). All mice underwent BP measurements followed by echocardiogram in week 6 after final surgery, and were then euthanized for tissue harvest and flow cytometry of blood and spleen cells. Marked reduction in T cell populations were noted in (B and C) thoracic lymph nodes and (D) spleen in mice treated with anti-CD3 antibody. Images in (B) were taken using a gross dissecting scope; scale bar represents 2 mm. Flow cytometry plots of (E) lymph node and (F) spleen are shown for representative samples from sham isotype, CKD isotype, and CKD anti-CD3 mice. Echocardiogram results are presented in (G), whereas BP and renal function are presented in (H). *P<0.05; **P<0.01; ***P<0.001. b, blood pressure; CysC, cystatin C; e, echocardiogram; FSC-A, forward scatter-area; iso, isotype control antibody; IVRT, isovolumic relaxation time; LV, left ventricular; MPI, myocardial performance index; S1, surgery 1; S2, surgery 2; SBP, systolic BP; x, end point.

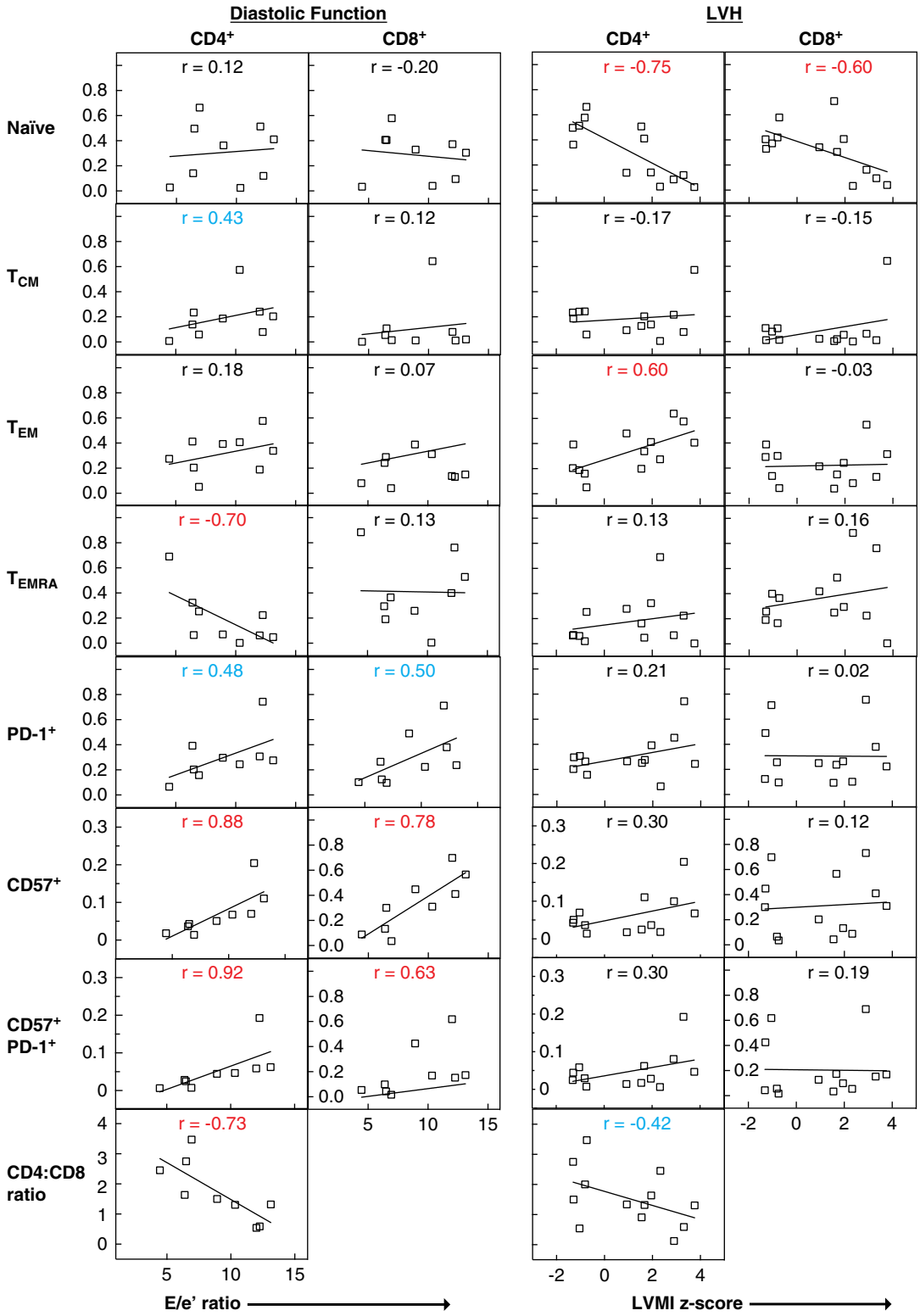

Figure 5. T cell populations with cardiac structure and function in children with CKD. Linear regression analysis of T cell populations reported in our previous study with diastolic function (E/e') and LVH (as defined by LVMI *z* score) in children with CKD. Moderate-strength associations (blue) were ascribed to those with Spearman correlation coefficient $r>0.4$, and strong associations (red) for $r>0.8$. E/e' ratio is a diastolic functional measure for which increasing ratio indicates worsening diastolic function. Memory cell subsets for this study were defined by the relative expression of CCR7 and CD45RA on $CD4^+$ and $CD8^+$ T cells isolated form peripheral blood as previously reported.[22] LVMI, height-indexed left ventricular mass ($g/m^{2.7}$); T_{CM}, central memory T cells; T_{EM}, effector memory T cells; T_{EMRA}, terminally differentiated effector memory $CD4^+$ T cells.

Appendix 8) between CKD mice receiving isotype control versus anti-CD3 antibody despite detectable differences in diastolic function and myocardial strain on echo. Therefore, fibrosis is unlikely the primary cause of early myocardial dysfunction in this model.

The mechanisms by which T cells affect myocardial dysfunction in this model remain to be determined. In addition to effective depletion of T cells, the use anti-CD3 antibody clone 145–2C11 has been shown to stimulate T cells *in vitro*[61] and result in acute cytokine release upon initial dose *in vivo*.[62] We were unable to detect TNF in undiluted plasma at 6 weeks of anti-CD3 treatment (see Figure 1 in Supplemental Appendix 8). The current data, in addition to the aforementioned studies in knockout mice, support the conclusion that reduced T cell number rather than sustained cytokine release mediated the improvement in cardiac function. Additional studies investigating the effect of modulating T cell activation and trafficking in this model are ongoing.

T cells express a myriad of inducible costimulatory and inhibitory signaling proteins during activation and differentiation to fine-tune the magnitude and character of an immune response.[63–65] In the context of chronic antigen stimulation, such as during persistent viral infections, sustained activation of T cells leads to depletion of naïve T cells and accumulation of terminally differentiated memory T cells that have proinflammatory characteristics.[66,67] Similar loss of naïve T cells and accumulation of memory T cells have been described in the peripheral blood of patients with CKD.[16,22] Here, we have demonstrated that the 5/6th nephrectomy mouse model of CKD recapitulates the T cell alterations described in patients with CKD.[68] Using both traditional flow cytometry gating and unsupervised clustering algorithms, we found loss of naïve $CD4^+$ T cells with accumulation of both central and effector memory cells bearing the coinhibitory signaling proteins PD-1 and KLRG1, and/or the costimulatory signaling protein OX40 in mice with CKD.

PD-1 is an inhibitory signaling protein induced on activated T cells that serves to control autoreactive immune responses during inflammation.[69,70] Genetic deficiencies or pharmacologic blockade of the PD-1 pathway have been implicated in several autoimmune diseases, including autoimmune myocarditis.[71,72] KLRG1 is postulated to be an inhibitory signaling receptor in antigen-experienced T cells and is dramatically upregulated on T cells during persistent antigen stimulation, such as during chronic viral infection.[73,74]

In the setting of chronic viral infection, expression of PD-1 and/or KLRG1 on T cells is associated with immune senescence characterized by impaired replicative and limited cytokine secretion capacities.[66,74] However, these receptors are also markers of T cell activation. Our data suggest this is the case in the CKD mouse model because T cells overall retained cytokine production capacity despite increased frequency of PD-1 and/or KLRG1 expression. We also found that T cells from uremic mice retain replicative capacity during *ex vivo* exposure to the mitogen phytohemagglutinin (data not shown). These data suggest that the T cell populations accumulating during CKD, although bearing markers of phenotypic activation/senescence, are capable of pathologic effects.

Similarly, expression of CD57 on human $CD8^+$ T cells is observed during persistent antigen stimulation as seen during chronic viral infections[75] and cancer.[76] In these clinical settings, $CD57^+$ T cells are functionally characterized by IFNγ secretion and increased susceptibility to activation-induced apoptosis and replicative senescence.[75,77] However, Espinosa *et al.*[78] recently demonstrated that $CD4^+CD57^+$ T cells collected from renal failure patients retained the capacity to both replicate and produce important cytokines for their function (IFNγ, TNF, Granzyme B) after *ex vivo* stimulation. We were unable to test the functionality of $CD57^+$ T cells in our historical pediatric cohort; however, the data presented justify further functional assessment these T cell populations and association with subclinical cardiovascular disease in patients with CKD.

In children with CKD, we found that diastolic function and LVH correlated with different T cell populations. Expression of the coinhibitory receptors PD-1 and CD57 were associated with diastolic function (E/e'), whereas loss of naïve T cells was associated with increasing left ventricular mass. Interestingly, T cell depletion in the mouse model of CKD, which improved diastolic function without improving LVH, also resulted in decreased absolute counts of circulating T cells bearing PD-1 or KLRG1 (data not shown). Conversely, in the pediatric cohort, accumulation of terminally differentiated $CD4^+$ memory T cells was associated with improving diastolic function. One possible explanation for this observation, which requires confirmation in future studies, is that the terminally differentiated $CD4^+$ memory T cell population represents functionally senescent cells that "lack the gas" to affect cardiac function. Interestingly, this memory subset contains a low frequency (approximately 1%) of cells expressing CD57.

We acknowledge that the associations between T cell populations and features of cardiomyopathy in pediatric patients with CKD presented here are limited because of the small sample size. We were nevertheless surprised to find Spearman correlation coefficients suggestive of moderate-to-strong associations despite this limitation, and plan to confirm these findings in a larger prospective cohort. Specific T cell populations may serve as novel biomarkers predictive of cardiovascular comorbidities. Furthermore, improved characterization of the T cell populations affecting early, subclinical myocardial dysfunction during CKD may inform development of novel therapies to mitigate cardiovascular morbidity and mortality in CKD.

ACKNOWLEDGMENTS

RNA sequencing was performed by the Yerkes National Primate Research Center Genomics Core (GenCore). The RNA sequencing data discussed in this publication have been deposited in the National Center for Biotechnology Information Gene Expression Omnibus[79]

and are accessible under the accession number GSE106385 (https://www.ncbi.nlm.nih.gov/geo/query/acc.cgi?acc=GSE106385).

P.D.W. and M.L.F. designed the experiments. J.M.R. analyzed and interpreted flow cytometry viSNE experiments. M.K. analyzed and interpreted biostatistics. R.P.G. designed, collected, and interpreted human flow cytometry data. P.D.W. and M.L.F. drafted and revised the manuscript. All authors approved the final version of the manuscript.

Work was supported by the following grants from the National Institutes of Health: K12 HD072245 and K08 DK111998 (to P.D.W.), and R01 AI073707 and R01 AI104699 (to M.L.F.). Support was also provided by the Children's Healthcare of Atlanta and Emory University's Pediatric Animal Physiology Core and Pediatric Biostatistics Core.

Preliminary data from this project was presented at the American Society for Nephrology Kidney Week in Chicago, IL, November 19, 2016.

DISCLOSURES

None.

SUPPLEMENTAL MATERIAL

This article contains the following supplemental material online at http://jasn.asnjournals.org/lookup/suppl/doi:10.1681/ASN.2017101138/-/DCSupplemental.

Supplemental Appendix 1. RNA sequencing normalized expression table (fragments per kilobase million) for each replicate sample as uploaded to Gene Expression Omnibus.

Supplemental Appendix 2. Differential expression analysis result table.

Supplemental Appendix 3. Ingenuity Pathway Analysis: biofunctions analysis with gene list (depicted in Figure 2).

Supplemental Appendix 4. Ingenuity Pathway Analysis: canonical pathways with gene list (depicted in Figure 2).

Supplemental Appendix 5. RNA sequencing confirmatory pathway analysis using DAVID algorithm.

Supplemental Appendix 6. Confirmatory Ingenuity Pathway Analysis: canonical pathway analysis with user dataset as reference background instead of default Ingenuity Pathway Analysis background.

Supplemental Appendix 7. Heatmap gene list with normalized expression as presented in Figure 2E.

Supplemental Appendix 8. Supplemental methods and analysis.

REFERENCES

1. Matteucci MC, Wühl E, Picca S, Mastrostefano A, Rinelli G, Romano C, et al.: ESCAPE Trial Group: Left ventricular geometry in children with mild to moderate chronic renal insufficiency. *J Am Soc Nephrol* 17: 218–226, 2006
2. Mitsnefes MM, Kimball TR, Border WL, Witt SA, Glascock BJ, Khoury PR, et al.: Impaired left ventricular diastolic function in children with chronic renal failure. *Kidney Int* 65: 1461–1466, 2004
3. Gruppen MP, Groothoff JW, Prins M, van der Wouw P, Offringa M, Bos WJ, et al.: Cardiac disease in young adult patients with end-stage renal disease since childhood: A Dutch cohort study. *Kidney Int* 63: 1058–1065, 2003
4. Chinali M, Matteucci MC, Franceschini A, Doyon A, Pongiglione G, Rinelli G, et al.: Advanced parameters of cardiac mechanics in children with CKD: The 4C study. *Clin J Am Soc Nephrol* 10: 1357–1363, 2015
5. Mathew J, Katz R, St John Sutton M, Dixit S, Gerstenfeld EP, Ghio S, et al.: Chronic kidney disease and cardiac remodelling in patients with mild heart failure: Results from the REsynchronization reVErses Remodeling in Systolic Left vEntricular Dysfunction (REVERSE) study. *Eur J Heart Fail* 14: 1420–1428, 2012
6. Krishnasamy R, Isbel NM, Hawley CM, Pascoe EM, Leano R, Haluska BA, et al.: The association between left ventricular global longitudinal strain, renal impairment and all-cause mortality. *Nephrol Dial Transplant* 29: 1218–1225, 2014
7. Liu YW, Su CT, Sung JM, Wang SP, Su YR, Yang CS, et al.: Association of left ventricular longitudinal strain with mortality among stable hemodialysis patients with preserved left ventricular ejection fraction. *Clin J Am Soc Nephrol* 8: 1564–1574, 2013
8. Cottone S, Nardi E, Mulè G, Vadalà A, Lorito MC, Riccobene R, et al.: Association between biomarkers of inflammation and left ventricular hypertrophy in moderate chronic kidney disease. *Clin Nephrol* 67: 209–216, 2007
9. Erten Y, Tulmac M, Derici U, Pasaoglu H, Altok Reis K, Bali M, et al.: An association between inflammatory state and left ventricular hypertrophy in hemodialysis patients. *Ren Fail* 27: 581–589, 2005
10. Espinoza M, Aguilera A, Auxiliadora Bajo M, Codoceo R, Caravaca E, Cirugeda A, et al.: Tumor necrosis factor alpha as a uremic toxin: Correlation with neuropathy, left ventricular hypertrophy, anemia, and hypertriglyceridemia in peritoneal dialysis patients. *Adv Perit Dial* 15: 82–86, 1999
11. Gupta J, Dominic EA, Fink JC, Ojo AO, Barrows IR, Reilly MP, et al.: CRIC Study Investigators: Association between inflammation and cardiac geometry in chronic kidney disease: Findings from the CRIC study. *PLoS One* 10: e0124772, 2015
12. Barreto DV, Barreto FC, Liabeuf S, Temmar M, Lemke HD, Tribouilloy C, et al.: European Uremic Toxin Work Group (EUTox): Plasma interleukin-6 is independently associated with mortality in both hemodialysis and predialysis patients with chronic kidney disease. *Kidney Int* 77: 550–556, 2010
13. Yeun JY, Levine RA, Mantadilok V, Kaysen GA: C-Reactive protein predicts all-cause and cardiovascular mortality in hemodialysis patients. *Am J Kidney Dis* 35: 469–476, 2000
14. Zimmermann J, Herrlinger S, Pruy A, Metzger T, Wanner C: Inflammation enhances cardiovascular risk and mortality in hemodialysis patients. *Kidney Int* 55: 648–658, 1999
15. Betjes MG, Langerak AW, van der Spek A, de Wit EA, Litjens NH: Premature aging of circulating T cells in patients with end-stage renal disease. *Kidney Int* 80: 208–217, 2011
16. Litjens NH, van Druningen CJ, Betjes MG: Progressive loss of renal function is associated with activation and depletion of naive T lymphocytes. *Clin Immunol* 118: 83–91, 2006
17. Lisowska KA, Dębska-Ślizień A, Jasiulewicz A, Heleniak Z, Bryl E, Witkowski JM: Hemodialysis affects phenotype and proliferation of CD4-positive T lymphocytes. *J Clin Immunol* 32: 189–200, 2012
18. Meier P, Dayer E, Blanc E, Wauters JP: Early T cell activation correlates with expression of apoptosis markers in patients with end-stage renal disease. *J Am Soc Nephrol* 13: 204–212, 2002
19. Yadav AK, Jha V: CD4+CD28null cells are expanded and exhibit a cytolytic profile in end-stage renal disease patients on peritoneal dialysis. *Nephrol Dial Transplant* 26: 1689–1694, 2011
20. Betjes MG, de Wit EE, Weimar W, Litjens NH: Circulating pro-inflammatory CD4posCD28null T cells are independently associated with cardiovascular disease in ESRD patients. *Nephrol Dial Transplant* 25: 3640–3646, 2010
21. Zhang J, Hua G, Zhang X, Tong R, Du X, Li Z: Regulatory T cells/T-helper cell 17 functional imbalance in uraemic patients on maintenance haemodialysis: A pivotal link between microinflammation and adverse cardiovascular events. *Nephrology (Carlton)* 15: 33–41, 2010
22. George RP, Mehta AK, Perez SD, Winterberg P, Cheeseman J, Johnson B, et al.: Premature T cell senescence in pediatric CKD. *J Am Soc Nephrol* 28: 359–367, 2017

23. Guzik TJ, Hoch NE, Brown KA, McCann LA, Rahman A, Dikalov S, et al.: Role of the T cell in the genesis of angiotensin II induced hypertension and vascular dysfunction. *J Exp Med* 204: 2449–2460, 2007
24. Madhur MS, Lob HE, McCann LA, Iwakura Y, Blinder Y, Guzik TJ, et al.: Interleukin 17 promotes angiotensin II-induced hypertension and vascular dysfunction. *Hypertension* 55: 500–507, 2010
25. Itani HA, McMaster WG Jr., Saleh MA, Nazarewicz RR, Mikolajczyk TP, Kaszuba AM, et al.: Activation of human T cells in hypertension: Studies of humanized mice and hypertensive humans. *Hypertension* 68: 123–132, 2016
26. Laroumanie F, Douin-Echinard V, Pozzo J, Lairez O, Tortosa F, Vinel C, et al.: CD4+ T cells promote the transition from hypertrophy to heart failure during chronic pressure overload. *Circulation* 129: 2111–2124, 2014
27. Nevers T, Salvador AM, Grodecki-Pena A, Knapp A, Velázquez F, Aronovitz M, et al.: Left ventricular T-cell recruitment contributes to the pathogenesis of heart failure. *Circ Heart Fail* 8: 776–787, 2015
28. Wu QQ, Yuan Y, Jiang XH, Xiao Y, Yang Z, Ma ZG, et al.: OX40 regulates pressure overload-induced cardiac hypertrophy and remodelling via CD4+ T-cells. *Clin Sci (Lond)* 130: 2061–2071, 2016
29. Nevers T, Salvador AM, Velazquez F, Ngwenyama N, Carrillo-Salinas FJ, Aronovitz M, et al.: Th1 effector T cells selectively orchestrate cardiac fibrosis in nonischemic heart failure. *J Exp Med* 214: 3311–3329, 2017
30. Winterberg PD, Jiang R, Maxwell JT, Wang B, Wagner MB: Myocardial dysfunction occurs prior to changes in ventricular geometry in mice with chronic kidney disease (CKD). *Physiol Rep* 4: e12732, 2016
31. Dobin A, Gingeras TR: Mapping RNA-seq reads with STAR. *Curr Protoc Bioinformatics* 51: 11.14.11–11.14.19, 2015
32. Trapnell C, Williams BA, Pertea G, Mortazavi A, Kwan G, van Baren MJ, et al.: Transcript assembly and quantification by RNA-Seq reveals unannotated transcripts and isoform switching during cell differentiation. *Nat Biotechnol* 28: 511–515, 2010
33. Amir AD, Davis KL, Tadmor MD, Simonds EF, Levine JH, Bendall SC, et al.: viSNE enables visualization of high dimensional single-cell data and reveals phenotypic heterogeneity of leukemia. *Nat Biotechnol* 31: 545–552, 2013
34. Golubovskaya V, Wu L: Different subsets of T cells, memory, effector functions, and CAR-T immunotherapy. *Cancers (Basel)* 8: 36, 2016
35. Mitter SS, Shah SJ, Thomas JD: A test in context: E/A and E/e' to assess diastolic dysfunction and LV filling pressure. *J Am Coll Cardiol* 69: 1451–1464, 2017
36. Khoury PR, Mitsnefes M, Daniels SR, Kimball TR: Age-specific reference intervals for indexed left ventricular mass in children. *J Am Soc Echocardiogr* 22: 709–714, 2009
37. Mair F, Hartmann FJ, Mrdjen D, Tosevski V, Krieg C, Becher B: The end of gating? An introduction to automated analysis of high dimensional cytometry data. *Eur J Immunol* 46: 34–43, 2016
38. Groothoff JW, Gruppen MP, Offringa M, Hutten J, Lilien MR, Van De Kar NJ, et al.: Mortality and causes of death of end-stage renal disease in children: A Dutch cohort study. *Kidney Int* 61: 621–629, 2002
39. Parekh RS, Carroll CE, Wolfe RA, Port FK: Cardiovascular mortality in children and young adults with end-stage kidney disease. *J Pediatr* 141: 191–197, 2002
40. Tonelli M, Wiebe N, Culleton B, House A, Rabbat C, Fok M, et al.: Chronic kidney disease and mortality risk: A systematic review. *J Am Soc Nephrol* 17: 2034–2047, 2006
41. Palmer SC, Navaneethan SD, Craig JC, Johnson DW, Perkovic V, Nigwekar SU, et al.: HMG CoA reductase inhibitors (statins) for dialysis patients. *Cochrane Database Syst Rev* CD004289, 2013
42. Drüeke TB, Locatelli F, Clyne N, Eckardt KU, Macdougall IC, Tsakiris D, et al.: CREATE Investigators: Normalization of hemoglobin level in patients with chronic kidney disease and anemia. *N Engl J Med* 355: 2071–2084, 2006
43. Eknoyan G, Beck GJ, Cheung AK, Daugirdas JT, Greene T, Kusek JW, et al.: Hemodialysis (HEMO) Study Group: Effect of dialysis dose and membrane flux in maintenance hemodialysis. *N Engl J Med* 347: 2010–2019, 2002
44. Jamison RL, Hartigan P, Kaufman JS, Goldfarb DS, Warren SR, Guarino PD, et al.: Veterans Affairs Site Investigators: Effect of homocysteine lowering on mortality and vascular disease in advanced chronic kidney disease and end-stage renal disease: A randomized controlled trial. *JAMA* 298: 1163–1170, 2007
45. Locatelli F, Aljama P, Canaud B, Covic A, De Francisco A, Macdougall IC, et al.: Anaemia Working Group of European Renal Best Practice (ERBP): Target haemoglobin to aim for with erythropoiesis-stimulating agents: A position statement by ERBP following publication of the Trial to reduce cardiovascular events with Aranesp therapy (TREAT) study. *Nephrol Dial Transplant* 25: 2846–2850, 2010
46. Zannad F, Kessler M, Lehert P, Grünfeld JP, Thuilliez C, Leizorovicz A, et al.: Prevention of cardiovascular events in end-stage renal disease: Results of a randomized trial of fosinopril and implications for future studies. *Kidney Int* 70: 1318–1324, 2006
47. Mitsnefes MM, Kimball TR, Kartal J, Witt SA, Glascock BJ, Khoury PR, et al.: Progression of left ventricular hypertrophy in children with early chronic kidney disease: 2-year follow-up study. *J Pediatr* 149: 671–675, 2006
48. Asp AM, Wallquist C, Rickenlund A, Hylander B, Jacobson SH, Caidahl K, et al.: Cardiac remodelling and functional alterations in mild-to-moderate renal dysfunction: Comparison with healthy subjects. *Clin Physiol Funct Imaging* 35: 223–230, 2015
49. Hayashi SY, Rohani M, Lindholm B, Brodin LA, Lind B, Barany P, et al.: Left ventricular function in patients with chronic kidney disease evaluated by colour tissue Doppler velocity imaging. *Nephrol Dial Transplant* 21: 125–132, 2006
50. Park M, Hsu CY, Li Y, Mishra RK, Keane M, Rosas SE, et al.: Chronic Renal Insufficiency Cohort (CRIC) Study Group: Associations between kidney function and subclinical cardiac abnormalities in CKD. *J Am Soc Nephrol* 23: 1725–1734, 2012
51. Cai QZ, Lu XZ, Lu Y, Wang AY: Longitudinal changes of cardiac structure and function in CKD (CASCADE study). *J Am Soc Nephrol* 25: 1599–1608, 2014
52. Panoulas VF, Sulemane S, Konstantinou K, Bratsas A, Elliott SJ, Dawson D, et al.: Early detection of subclinical left ventricular myocardial dysfunction in patients with chronic kidney disease. *Eur Heart J Cardiovasc Imaging* 16: 539–548, 2015
53. Krishnasamy R, Isbel NM, Hawley CM, Pascoe EM, Burrage M, Leano R, et al.: Left ventricular global longitudinal strain (GLS) is a superior predictor of all-cause and cardiovascular mortality when compared to ejection fraction in advanced chronic kidney disease. *PLoS One* 10: e0127044, 2015
54. Redfield MM, Jacobsen SJ, Burnett JC Jr., Mahoney DW, Bailey KR, Rodeheffer RJ: Burden of systolic and diastolic ventricular dysfunction in the community: Appreciating the scope of the heart failure epidemic. *JAMA* 289: 194–202, 2003
55. Aeschbacher BC, Hutter D, Fuhrer J, Weidmann P, Delacrétaz E, Allemann Y: Diastolic dysfunction precedes myocardial hypertrophy in the development of hypertension. *Am J Hypertens* 14: 106–113, 2001
56. Di Bello V, Talini E, Dell'Omo G, Giannini C, Delle Donne MG, Canale ML, et al.: Early left ventricular mechanics abnormalities in prehypertension: A two-dimensional strain echocardiography study. *Am J Hypertens* 23: 405–412, 2010
57. Dupont S, Maizel J, Mentaverri R, Chillon JM, Six I, Giummelly P, et al.: The onset of left ventricular diastolic dysfunction in SHR rats is not related to hypertrophy or hypertension. *Am J Physiol Heart Circ Physiol* 302: H1524–H1532, 2012
58. Salzler HR, Griffiths R, Ruiz P, Chi L, Frey C, Marchuk DA, et al.: Hypertension and albuminuria in chronic kidney disease mapped to a mouse chromosome 11 locus. *Kidney Int* 72: 1226–1232, 2007
59. Ma LJ, Fogo AB: Model of robust induction of glomerulosclerosis in mice: Importance of genetic background. *Kidney Int* 64: 350–355, 2003
60. Siedlecki AM, Jin X, Muslin AJ: Uremic cardiac hypertrophy is reversed by rapamycin but not by lowering of blood pressure. *Kidney Int* 75: 800–808, 2009
61. Beyersdorf N, Braun A, Vögtle T, Varga-Szabo D, Galdos RR, Kissler S, et al.: STIM1-independent T cell development and effector function in vivo. *J Immunol* 182: 3390–3397, 2009

62. Alegre ML, Vandenabeele P, Depierreux M, Florquin S, Deschodt-Lanckman M, Flamand V, et al.: Cytokine release syndrome induced by the 145-2C11 anti-CD3 monoclonal antibody in mice: Prevention by high doses of methylprednisolone. *J Immunol* 146: 1184–1191, 1991
63. Jameson SC, Masopust D: Diversity in T cell memory: An embarrassment of riches. *Immunity* 31: 859–871, 2009
64. Ford ML: T cell cosignaling molecules in transplantation. *Immunity* 44: 1020–1033, 2016
65. Granier C, De Guillebon E, Blanc C, Roussel H, Badoual C, Colin E, et al.: Mechanisms of action and rationale for the use of checkpoint inhibitors in cancer. *ESMO Open* 2: e000213, 2017
66. Wherry EJ, Ha SJ, Kaech SM, Haining WN, Sarkar S, Kalia V, et al.: Molecular signature of CD8+ T cell exhaustion during chronic viral infection. *Immunity* 27: 670–684, 2007
67. Appay V, Sauce D: Immune activation and inflammation in HIV-1 infection: Causes and consequences. *J Pathol* 214: 231–241, 2008
68. Costa E, Lima M, Alves JM, Rocha S, Rocha-Pereira P, Castro E, et al.: Inflammation, T-cell phenotype, and inflammatory cytokines in chronic kidney disease patients under hemodialysis and its relationship to resistance to recombinant human erythropoietin therapy. *J Clin Immunol* 28: 268–275, 2008
69. Okazaki T, Honjo T: The PD-1-PD-L pathway in immunological tolerance. *Trends Immunol* 27: 195–201, 2006
70. Sharpe AH, Wherry EJ, Ahmed R, Freeman GJ: The function of programmed cell death 1 and its ligands in regulating autoimmunity and infection. *Nat Immunol* 8: 239–245, 2007
71. Tarrio ML, Grabie N, Bu DX, Sharpe AH, Lichtman AH: PD-1 protects against inflammation and myocyte damage in T cell-mediated myocarditis. *J Immunol* 188: 4876–4884, 2012
72. Nishimura H, Okazaki T, Tanaka Y, Nakatani K, Hara M, Matsumori A, et al.: Autoimmune dilated cardiomyopathy in PD-1 receptor-deficient mice. *Science* 291: 319–322, 2001
73. Ibegbu CC, Xu YX, Harris W, Maggio D, Miller JD, Kourtis AP: Expression of killer cell lectin-like receptor G1 on antigen-specific human CD8+ T lymphocytes during active, latent, and resolved infection and its relation with CD57. *J Immunol* 174: 6088–6094, 2005
74. Thimme R, Appay V, Koschella M, Panther E, Roth E, Hislop AD, et al.: Increased expression of the NK cell receptor KLRG1 by virus-specific CD8 T cells during persistent antigen stimulation. *J Virol* 79: 12112–12116, 2005
75. Brenchley JM, Karandikar NJ, Betts MR, Ambrozak DR, Hill BJ, Crotty LE, et al.: Expression of CD57 defines replicative senescence and antigen-induced apoptotic death of CD8+ T cells. *Blood* 101: 2711–2720, 2003
76. Sze DM, Giesajtis G, Brown RD, Raitakari M, Gibson J, Ho J, et al.: Clonal cytotoxic T cells are expanded in myeloma and reside in the CD8(+)CD57(+)CD28(-) compartment. *Blood* 98: 2817–2827, 2001
77. Bandrés E, Merino J, Vázquez B, Inogés S, Moreno C, Subirá ML, et al.: The increase of IFN-gamma production through aging correlates with the expanded CD8(+high)CD28(-)CD57(+) subpopulation. *Clin Immunol* 96: 230–235, 2000
78. Espinosa J, Herr F, Tharp G, Bosinger S, Song M, Farris AB 3rd, et al.: CD57(+) CD4 T cells underlie belatacept-resistant allograft rejection. *Am J Transplant* 16: 1102–1112, 2016
79. Barrett T, Wilhite SE, Ledoux P, Evangelista C, Kim IF, Tomashevsky M, et al.: NCBI GEO: Archive for functional genomics data sets--update. *Nucleic Acids Res* 41: D991–D995, 2013